examples), although it is difficult to assign a simple interpretation to the magnitude of this statistic.

The second Donoho–Johnstone synthetic signal is shown in Fig. 2(a). This signal is qualitatively similar to a nuclear magnetic resonance spectrum. The corresponding noisy signal is shown in Fig. 2(b). The LSM reconstruction is shown in Fig. 2(c), whereas the wavelet shrinkage reconstruction is shown in Fig. 2(d). Comparing the individual peaks in the two reconstructed signals with the corresponding peaks in the noise-free signal, it is clear that the LSM method yields quantitatively superior results in addition to producing a visually pleasing reconstruction.

Fig. 3(a) shows the third Donoho–Johnstone synthetic signal consisting of a sine wave that is divided into two parts with the second part shifted upwards by a constant amount. The corresponding noisy signal is shown in Fig. 3(b). The LSM reconstruction is shown in Fig. 3(c), and the wavelet shrinkage reconstruction is shown in Fig. 3(d).

Finally, Fig. 4(a) shows the fourth Donoho–Johnstone synthetic signal, which is sinusoidal with the frequency increasing rapidly toward the origin. Fig. 4(c) and (d) display the LSM reconstruction and the wavelet shrinkage reconstruction, respectively. These reconstructions were based on the noisy signal shown in Fig. 4(b).

III. Discussion

In this correspondence, we have introduced the concept of the *local smoothness map*, which is a generalization of the *global smoothness parameter* that is commonly used to stabilize inverse problems. The Bayesian approach to finding the optimal local smoothness map allows us to accurately recover sharp gradients in the original signal whenever the data strongly supports the existence of such discontinuities. We have demonstrated the effectiveness of the new method on the classic problem of denoising one-dimensional signals. Further applications to problems involving nontrivial point-spread functions and two-dimensional data have yielded promising results that will be reported elsewhere.

References

[1] A. M. Thompson, J. C. Brown, J. W. Kay, and D. M. Titterington, "A study of methods for choosing the smoothing parameter in image restoration by regularization," *IEEE Trans. Pattern Anal. Machine Intell.*, vol. 13, p. 326–339, 1991.

[2] W. H. Press, S. A. Teukolsky, B. P. Flannery, and W. T. Vetterling, *Numerical Recipes in C*. Cambridge, U.K.: Cambridge Univ. Press, 1992, p. 627.

[3] D. Donoho and I. Johnstone, "Adapting to unknown smoothness via wavelet shrinkage," Tech. Rep. 425, Dept. Statist., Stanford Univ, Stanford, CA, June 1993.

[4] C. Chui, *Wavelets*. New York: Academic, 1992.

The Eigenvalues of Matrices that Occur in Certain Interpolation Problems

Paulo J. S. G. Ferreira

***Abstract*—The eigenvalues of the matrices that occur in certain finite-dimensional interpolation problems are directly related to their well posedness and strongly depend on the distribution of the interpolation knots, that is, on the sampling set. We study this dependency as a function of the sampling set itself and give accurate bounds for the eigenvalues of the interpolation matrices. The bounds can be evaluated in as few as four arithmetic operations, and therefore, they greatly simplify the assessment of sampling sets regarding numerical stability. The accuracy and usefulness of the bounds are illustrated with examples.**

I. Introduction

One problem commonly found in signal processing is that of recovering n lost samples of a bandlimited discrete signal with a total of N samples. The Papoulis–Gerchberg algorithm [1], [2], although initially developed for extrapolation problems, is a well-known example of an iterative technique that can be used to solve this problem. It is related to a number of other methods, including alternating projections [3] and POCS [4]–[6]. These projection methods may outperform the basic iteration since they allow any number of *a priori* constraints to be included in the problem.

Many other works have subsequently dealt with different aspects of the finite- or infinite-dimensional interpolation problem. Sampled bandlimited L_2 functions can be interpolated using an iterative algorithm [7], [8] related to the Papoulis–Gerchberg method. The interpolation of bandlimited signals from finite sets of nonuniform samples was studied in [9] and [10], among other works. The noniterative method studied in [11] and [12] is also valid for L_2 functions that are integral transforms of compactly supported functions [13]. Specific aspects of the finite-dimensional interpolation problem are discussed in [14]–[17]. See [15] for a survey of some other closely related topics and references.

This correspondence was motivated by the following observations. It has been noticed that the finite-dimensional interpolation problem can be reduced to the solution of a linear set of equations with a real, symmetric positive-definite $n \times n$ matrix $\mathbf{S}$, with spectral radius $\rho(\mathbf{S})$ less than unity [18]. This immediately yields noniterative and iterative solutions to the problem, which, however, may be ill-conditioned, leading to serious practical difficulties. These difficulties are shared by the finite-dimensional version of the Papoulis–Gerchberg algorithm [15], where the impact of ill condititiong is felt in the slow convergence rates.

However, the stability of the interpolation problem critically depends on the sampling set. For both iterative and noniterative methods, assessment of the sampling sets is a crucial task. A number of results concerning this topic have been published. The performance of the finite-dimensional Papoulis-Gerchberg algorithm as a function of the sampling set was studied in [15]. Reference [19] addresses the interpolation of continuous-time signals from incomplete sets of samples. The goal in [20] is to minimize the maximum of the mean-squared error over a class of images with respect to the sampling set.

Manuscript received August 26, 1994; revised April 1, 1997. This work was supported in part by JNICT. The associate editor coordinating the review of this paper and approving it for publication was Prof. José M. F. Moura.

The author is with Department of Electrónica e Telecomunicações, INESC, Universidade de Aveiro, Aveiro, Portugal (e-mail: pjf@inesca.pt).

Publisher Item Identifier S 1053-587X(97)05797-8.

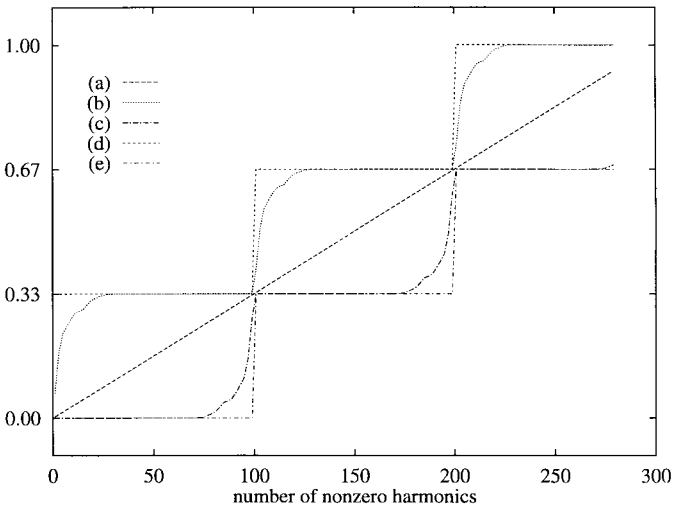

Fig. 1. Eigenvalues of $\mathbf{S}$ and their bounds, for the lowpass case, as a function of the bandwidth $2m+1$. $N=300$, $n=20$, and $k=3$. (a) Line $(2m+1)/N$, Theorem 1. (b), (c) Upper/lower bounds, Theorem 2. (d), (e) Largest/smallest eigenvalues.

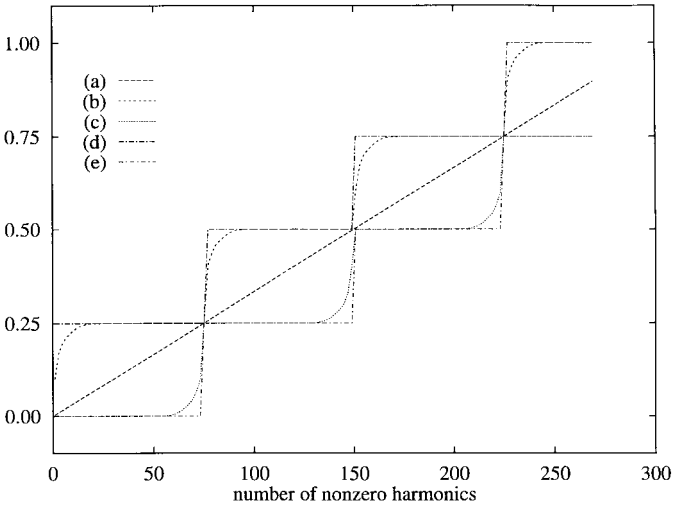

Fig. 2. Eigenvalues of $\mathbf{S}$ and their bounds, for the lowpass case, as a function of the bandwidth $2m+1$. $N=300$, $n=30$, and $k=4$. (a) Line $(2m+1)/N$, Theorem 1. (b, (c) Upper/lower bounds, Theorem 2. (d), (e) Largest/smallest eigenvalues.

In these works, it was concluded that for some types of passbands, the optimum performance of the interpolation process is achieved for equidistant sampling points.

In this correspondence, we give accurate bounds for the eigenvalues of the interpolation matrices, the simplest of which can be found in $O(1)$ time, using only four arithmetic operations. Even the more complex can be found in $O(n)$ time. This dramatically simplifies the assessment of the sampling sets in this class of interpolation problems, yielding precise, quantitative numerical stability measures. It also explains the striking staircase-like behavior of the eigenvalues, which are illustrated in Figs. 1 and 2. The paper closes with a few examples and applications that demonstrate the effectiveness and accuracy of the bounds.

II. Results

We work in $\mathbb{C}^N$, and thus, all signals considered are vectors in N-dimensional space. A signal is bandlimited if its discrete Fourier transform has a proper subset of zero samples. A sampling set U is a subset of $\{0,1,\ldots,N-1\}$ with $0<n<N$ distinct elements

$$U=\{i_0,i_1,\ldots,i_{n-1}\}.$$

The finite-dimensional bandlimited interpolation problem consists of restoring the samples x_i ($i\in U$) of a bandlimited discrete signal, using the remaining ones. It is known [18] that the problem can be reduced to the equation

$$\mathbf{u}=\mathbf{S}\mathbf{u}+\mathbf{h} \tag{1}$$

where $\mathbf{u}$ is the $n\times 1$ vector of unknown samples, the $n\times 1$ vector $\mathbf{h}$ depends only on the known samples, and $\mathbf{S}$ is a $n\times n$ matrix. If the nonzero harmonics of the signal are numbered a through b, the elements of $\mathbf{S}$ are

$$\begin{aligned} S_{pq} &= \frac{1}{N}\sum_{\ell=a}^{b} e^{j\frac{2\pi}{N}(i_p-i_q)\ell} \\ &= e^{j\frac{\pi}{N}(i_p-i_q)(b+a)}\,\frac{\sin[\pi(b-a+1)(i_p-i_q)/N]}{N\sin[\pi(i_p-i_q)/N]} \end{aligned} \tag{2}$$

when $p\neq q$. The diagonal elements S_{ii} are $(b-a+1)/N$. This quantity can be interpreted as a normalized bandwidth and will be denoted by B from now on.

Note that $\mathbf{S}$ is Hermitian. The most important special case is that of lowpass signals bandlimited to $2m+1$ nonzero harmonics, which is obtained by setting $a=-m$ and $b=m$.

The quadratic form associated with $\mathbf{S}$ is

$$\begin{aligned} \mathbf{x}^H\mathbf{S}\mathbf{x} &= \sum_{p=0}^{n-1}\sum_{q=0}^{n-1} x_p^* x_q\left[\frac{1}{N}\sum_{\ell=a}^{b} e^{j\frac{2\pi}{N}(i_p-i_q)\ell}\right] \\ &= \sum_{\ell=a}^{b}\left|\frac{1}{\sqrt{N}}\sum_{p=0}^{n-1} x_p e^{-j\frac{2\pi}{N}i_p\ell}\right|^2. \end{aligned}$$

We use the notation

$$\mathbf{x}^H\mathbf{S}\mathbf{x}=\sum_{\ell=a}^{b}|\phi(\ell)|^2 \tag{3}$$

where

$$\phi(\ell)=\frac{1}{\sqrt{N}}\sum_{p=0}^{n-1} x_p e^{-j\frac{2\pi}{N}i_p\ell}.$$

We are interested in $\mathbf{S}$ and its eigenvalues as functions of the sampling set U. To emphasize this, we write $\mathbf{S}(U)$ whenever convenient, or, even more explicitly, $\mathbf{S}(\{i_0,i_1,\ldots,i_{n-1}\})$. Thus, for example, $\mathbf{S}(\{0,3,8\})$ is the 3×3 matrix that arises in the recovery of samples x_0, x_3, and x_8 of a bandlimited signal.

It is a consequence of (3) that the eigenvalues of $\mathbf{S}$ are nonnegative. In fact, since the $N\times N$ filtering matrix $\mathbf{B}=\mathbf{S}(\{0,1,\ldots,N-1\})$ with elements

$$B_{pq}=e^{j\frac{\pi}{N}(p-q)(b+a)}\,\frac{\sin[\pi(b-a+1)(p-q)/N]}{N\sin[\pi(p-q)/N]} \tag{4}$$

has eigenvalues $\lambda=0$ or $\lambda=1$ only, $\mathbf{S}$, being a $n\times n$ principal submatrix of $\mathbf{B}$, has all its eigenvalues in the interval $[0,1]$. This follows straightforwardly, for example, from the interlacing inequalities [21].

It is also known (see [18]) that $\mathbf{I}-\mathbf{S}$ is nonsingular if the density of the known samples $(N-n)/N$ exceeds the bandwidth $B=(b-a+1)/N$ of the data and if $\mathbf{B}$ has contiguous eigenvalues (this is the case for lowpass and highpass signals, for example).

We now proceed to study the dependence of the eigenvalues of $\mathbf{S}(U)$ on the sampling set U.

Theorem 1: The minimum eigenvalue $\lambda_{\min}$ of $\mathbf{S}$ belongs to $[0,B]$ and the maximum eigenvalue $\lambda_{\max}$ to $[B,1]$, with $B=(b-a+1)/N$.

Proof: The proof is a consequence of

$$n\lambda_{\min} \le \sum_{i=1}^{n} \lambda_i = nB \le n\lambda_{\max}.$$

□

The simplest possible structure for U is considered in the following theorem, where, as usual, $\lfloor x \rfloor$ denotes the largest integer smaller than or equal to x, and $\lceil x \rceil$ denotes the smallest integer greater than or equal to x.

Theorem 2: If $U = \{i_0 k, i_1 k, \ldots, i_{n-1} k\}$, and N/k is an integer, the smallest and largest eigenvalues $\lambda_{\min}$ and $\lambda_{\max}$ of the matrix $\mathbf{S}(U)$ defined by (2) satisfy

$$\frac{\lfloor kB \rfloor}{k} \le \lambda_{\min} \le \lambda_{\max} \le \frac{\lceil kB \rceil}{k}$$

where $B = (b - a + 1)/N$.

Proof: The theorem gives trivial bounds if $k = 1$, and therefore, we assume that $k > 1$. Consider the matrix $\mathbf{S}$ as a function of a and b. Clearly, $\mathbf{S}$ will be diagonal if and only if $(b - a + 1)k/N$ is an integer. The smallest value of $b - a + 1$ for which this happens is

$$b - a + 1 = \frac{N}{k}. \tag{5}$$

Under the conditions of the theorem, there exist integers a and b that solve this equation and for which $S_{ii} = (b-a+1)/N = 1/k$. Thus, when (5) holds

$$\mathbf{x}^H \mathbf{S} \mathbf{x} = \frac{1}{k} \sum_{i=0}^{n-1} |x_i|^2$$

which means that

$$\sum_{\ell=a}^{b} |\phi(\ell)|^2 = \frac{1}{k} \sum_{i=0}^{n-1} |x_i|^2. \tag{6}$$

Now, let $0 < b - a + 1 < N$. Under the hypothesis placed on U, ϕ is periodic with period N/k. The interval $[a, b]$ contains at least

$$\left\lfloor \frac{b - a + 1}{N/k} \right\rfloor$$

periods of ϕ and at most

$$\left\lceil \frac{b - a + 1}{N/k} \right\rceil$$

periods of the same function. This and (6) implies

$$\mathbf{x}^H \mathbf{S} \mathbf{x} = \sum_{\ell=a}^{b} |\phi(\ell)|^2 \ge \frac{\lfloor kB \rfloor}{k} \sum_{i=0}^{n-1} |x_i|^2$$

$$\mathbf{x}^H \mathbf{S} \mathbf{x} = \sum_{\ell=a}^{b} |\phi(\ell)|^2 \le \frac{\lceil kB \rceil}{k} \sum_{i=0}^{n-1} |x_i|^2.$$

However, the smallest and largest eigenvalues of $\mathbf{S}$ are, respectively, equal to the minimum and maximum values assumed by $\mathbf{x}^T \mathbf{S} \mathbf{x}$, subject to $\|\mathbf{x}\| = 1$. □

The bounds can be found in negligible time (they require only a total of four arithmetic operations, including the rounding operation and the computation of B). Nevertheless, as the examples subsequently given will confirm, they are quite accurate and can be combined with those of Theorem 1.

We now turn to arbitrary sampling sets.

Theorem 3: Let $U_n = \{i_0, i_1, \ldots, i_{n-1}\}$ and $U_{n-1} = \{i_0, i_1, \ldots, i_{n-2}\}$. Denote by $\mathbf{S}_n$ and $\mathbf{S}_{n-1}$ the $n \times n$ and $(n-1) \times (n-1)$ interpolation matrices associated with the sampling sets U_n and U_{n-1}, respectively. Then

$$\lambda'(\mathbf{S}_{n-1}) - \|\mathbf{v}\| \le \lambda(\mathbf{S}_n) \le \lambda'(\mathbf{S}_{n-1}) + \|\mathbf{v}\| \tag{7}$$

where the vector $\mathbf{v}$ is defined by

$$v_k = e^{j\frac{\pi}{N}(i_k - i_{n-1})(b+a)} \frac{\sin[\pi(b-a+1)(i_k - i_{n-1})/N]}{N \sin[\pi(i_k - i_{n-1})/N]} \tag{8}$$

for $0 \le k \le n-2$. $\lambda'(\mathbf{S}_{n-1})$ denotes the sequence of the eigenvalues of $\mathbf{S}_{n-1}$, together with B, sorted by increasing order, and $\lambda(\mathbf{S}_n)$ stands for the eigenvalues of $\mathbf{S}_n$, ordered in the same way.

Proof: Express $\mathbf{S}_n$ as

$$\mathbf{S}_n = \left[\begin{array}{c|c} \mathbf{S}_{n-1} & 0 \\ \hline 0 & B \end{array}\right] + \left[\begin{array}{c|c} 0 & \mathbf{v} \\ \hline \mathbf{v}^H & 0 \end{array}\right]$$

where, according to (2), $B = (b - a + 1)/N$, and the v_k, $0 \le k \le n - 2$ are given by (8). The eigenvalues of the first of these two matrices are those of $\mathbf{S}_{n-1}$, together with B. When sorted by increasing order, these numbers become the $\lambda'(\mathbf{S}_{n-1})$ referred to in the theorem. The nonzero eigenvalues of the second matrix are $\pm\|\mathbf{v}\|$. It follows from Weyl's theorem on the eigenvalues of the sum of two Hermitian matrices [21] that the ordered eigenvalues $\lambda(\mathbf{S}_n)$ satisfy (7). □

Note that $\|\mathbf{v}\|$ can be computed using $O(n)$ operations. This result is useful for sampling sets that can be expressed as $U = U_1 \cup U_2$, where U_1 is of the type addressed by Theorem 2, and U_2 is arbitrary. The simplest possible case arises when U_2 has a single element (consider, for example, $U = \{0, 4, 12, 17\}$). In these cases, the theorem can be directly applied. If U_2 has more than one element, the theorem may be applied once for each element.

Corollary 1: The smallest and largest eigenvalues $\lambda_{\min}(\mathbf{S}_n)$ and $\lambda_{\max}(\mathbf{S}_n)$ of $\mathbf{S}_n$ satisfy

$$\lambda_{\min}(\mathbf{S}_n) \ge \lambda_{\min}(\mathbf{S}_{n-1}) - \|\mathbf{v}\|$$

$$\lambda_{\max}(\mathbf{S}_n) \le \lambda_{\max}(\mathbf{S}_{n-1}) + \|\mathbf{v}\|.$$

Proof: The equations in (7) imply that

$$\lambda_{\min}(\mathbf{S}_n) \ge \min\left[\lambda_{\min}(\mathbf{S}_{n-1}), B\right] - \|\mathbf{v}\|$$

$$\lambda_{\max}(\mathbf{S}_n) \le \max\left[\lambda_{\max}(\mathbf{S}_{n-1}), B\right] + \|\mathbf{v}\|.$$

By Theorem 1

$$0 \le \lambda_{\min}(\mathbf{S}_{n-1}) \le B$$

$$B \le \lambda_{\max}(\mathbf{S}_{n-1}) \le 1.$$

Thus

$$\min\left[\lambda_{\min}(\mathbf{S}_{n-1}), B\right] = \lambda_{\min}(\mathbf{S}_{n-1})$$

$$\max\left[\lambda_{\max}(\mathbf{S}_{n-1}), B\right] = \lambda_{\max}(\mathbf{S}_{n-1}).$$

□

Corollary 2: There exists an eigenvalue λ of $\mathbf{S}_n$ such that $B - \|\mathbf{v}\| \le \lambda \le B + \|\mathbf{v}\|$.

Proof: Select, from (7), the one that corresponds to $\lambda'(\mathbf{S}_{n-1}) = B$. □

Lemma 1: The Euclidean norm of the $(n-1)$-dimensional vector $\mathbf{v}$ defined by (8), for $0 \le k \le n-2$, satisfies $\|\mathbf{v}\|^2 \le B(1-B)$, where $B = (b - a + 1)/N$.

Proof: The $N \times N$ matrix $\mathbf{B}$ defined by (4) is idempotent, that is, it satisfies $\mathbf{B}^2 = \mathbf{B}$. Let $\mathbf{B}_i$ denote its ith column. Since the matrix is Hermitian, its ith line equals $\mathbf{B}_i^H$. The idempotency means that $\mathbf{B}_i^H \mathbf{B}_j = B_{ij}$. The squared norm of any of the $\mathbf{B}_i$ is therefore B_{ii}, which equals B ($\mathbf{B}_i^H \mathbf{B}_i = \|\mathbf{B}_i\|^2 = B_{ii} = B$).

The vector $\mathbf{v}$ is obtained from column i_{n-1} of $\mathbf{B}$ through the removal of $N - n + 1$ elements, including the diagonal element. Thus, $B^2 + \|\mathbf{v}\|^2 \le B$. □

Corollary 3: The bounds of Theorem 3 may be replaced by the weaker bounds

$$\lambda'(\mathbf{S}_{n-1}) - \sqrt{B(1-B)} \le \lambda(\mathbf{S}_n) \le \lambda'(\mathbf{S}_{n-1}) + \sqrt{B(1-B)}$$

where $B = (b - a + 1)/N$.

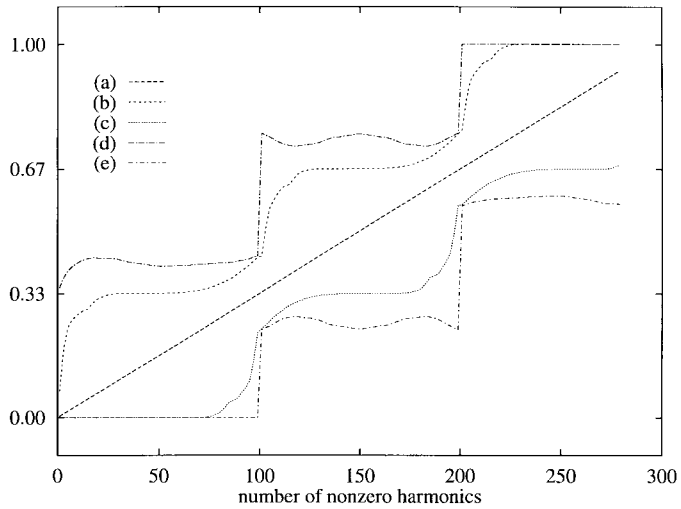

Fig. 3. Eigenvalues of $\mathbf{S}$ and their bounds, for the lowpass case, as a function of the bandwidth $2m + 1. N = 300, n = 21$,. (a) Line $(2m + 1)/N$, Theorem 1. (b), (c) Upper/lower bounds, Theorem 3. (d), (e) Largest/smallest eigenvalues.

Proof: The proof is an immediate consequence of Theorem 3 and Lemma 1. □

An argument similar to the one employed in the proof of Corollary 1 shows that this implies that the smallest and largest eigenvalues $\lambda_{\min}(\mathbf{S}_n)$ and $\lambda_{\max}(\mathbf{S}_n)$ of $\mathbf{S}_n$ satisfy the weaker inequalities

$$\lambda_{\min}(\mathbf{S}_n) \geq \lambda_{\min}(\mathbf{S}_{n-1}) - \sqrt{B(1-B)}$$
$$\lambda_{\max}(\mathbf{S}_n) \leq \lambda_{\max}(\mathbf{S}_{n-1}) + \sqrt{B(1-B)}.$$

III. Examples

We now present some examples that demonstrate the effectiveness of the bounds. Figs. 1–4 depict the largest and smallest eigenvalues of the matrix $\mathbf{S}$ defined by (2) as functions of the bandwidth, together with the upper and lower bounds given by Theorem 2.

The figures refer to lowpass data with $2m + 1$ nonzero harmonics, in which case, $a = -m$, and $b = m$. The reconstruction problem ceases to have a solution if $N - n \leq 2m + 1$ (see [18]). Thus, only values of m that satisfy this relation were considered.

Theorem 1 asserts that the largest and smallest eigenvalues of $\mathbf{S}$, as a function of m, are separated by the line $(2m + 1)/N$. This line is also depicted in the figures.

The number of missing samples and, consequently, the order of the matrices varies among the figures. The set of missing samples, in the case of Fig. 1, has 20 elements

$$U_1 = \{0, 3, 9 - 21, 33 - 45, 51 - 69, 75\}.$$

The notation a-b stands for $\{a, a+3, a+6, \ldots, b\}$. The set of missing samples to which Fig. 2 refers has 30 elements, which are

$$U_2 = 0, 4, 12 - 20, 28 - 40, 64, 68, 76, 80$$
$$88 - 120, 128, 132, 140, 144, 152 - 168\}.$$

Now, a-b is shorthand for $\{a, a + 4, a + 8, \ldots, b\}$. The missing samples are, in the first case, multiples of 3 and, in the second case, multiples of 4. Consequently, Theorem 2 applies in both cases.

The bounds would be even sharper if the missing samples formed an arithmetic progression without gaps or if the number of missing samples is increased. In many cases, the bounds are rather approximate estimates of the extreme eigenvalues of the matrix $\mathbf{S}$ in (1). To keep the figures readable, we deliberately avoided those cases.

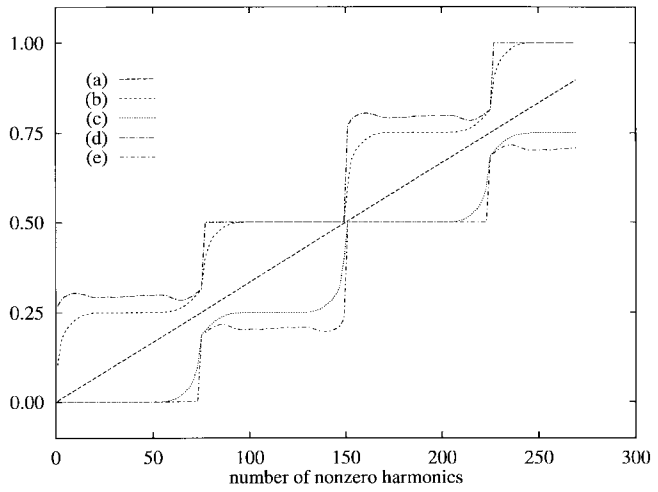

Fig. 4. Eigenvalues of $\mathbf{S}$ and their bounds, for the lowpass case, as a function of the bandwidth $2m + 1. N = 300, n = 31$,. (a) Line $(2m + 1)/N$, Theorem 1. (b), (c) Upper/lower bounds, Theorem 2 and Theorem 3. (d), (e) Largest/smallest eigenvalues.

The sampling sets U_3 and U_4 to which Figs. 3 and 4 refer are given by

$$U_3 = U_1 \cup \{28\}, \quad U_4 = U_2 \cup \{50\}.$$

Theorem 2 cannot be applied to U_3 since the greatest common divider of the elements of U_3 is unitary. Therefore, the bounds depicted in Fig. 3 are those that follow from Theorem 3.

In the last example, whichis depicted in Fig. 4, the element 50, which is added to the set U_2, caused the greatest common divider to drop from 4 to 2. Thus, Theorem 2 may still be applied, although with $k = 2$ instead of $k = 4$. It is, of course, also possible to apply Theorem 3 as well, and in fact, the bounds depicted are the intersection of the two.

IV. Applications

A. Estimating the Optimum Relaxation Parameter

Equation (1) can be solved to the desired accuracy using iterative techniques, whose performance generally depends on the value of a relaxation parameter. The explicit expression for the optimum value of the parameter in the finite-dimensional Papoulis–Gerchberg algorithm is given in [15].

Unfortunately, the computation of the optimum value of the relaxation parameter often depends on knowing the eigenvalues of certain matrices: either the iteration matrices themselves or some other closely related matrix. For ill-posed or large problems, determination of the eigenvalues may be difficult or time consuming. On the other hand, iteration with a suboptimum relaxation parameter may yield comparatively low convergence rates.

The bounds given in this paper can be used to find approximate values for the eigenvalues of the iteration matrices of some of the iterations discussed in [18] or to estimate the condition number of the matrix $\mathbf{S}$ in (1). This gives a quantitative measure of the feasibility of the reconstruction problem itself with an extra bonus: The approximations to the eigenvalues may lead to near optimum relaxation parameters.

Consider, for example, the iterative method

$$\mathbf{x}_{i+1} = \mu(\mathbf{S}\mathbf{x}_i + \mathbf{h}) + (1 - \mu)\mathbf{x}_i \tag{9}$$

which is equivalent to

$$\mathbf{x}_{i+1} = [(1 - \mu)\mathbf{I} + \mu\mathbf{S}]\mathbf{x}_i + \mu\mathbf{h}.$$

We write $\mathbf{S}_\mu = (1 - \mu)\mathbf{I} + \mu\mathbf{S}$. When $\mu = 1$, the method reduces to

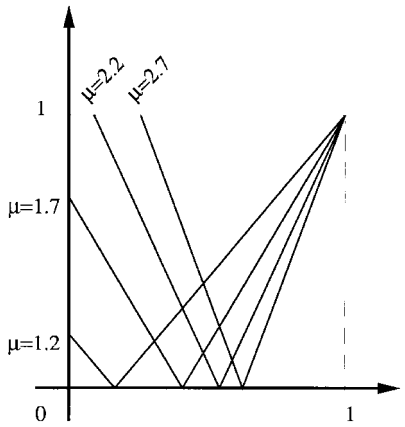

Fig. 5. Absolute value of the functions $f_\mu(x) = 1 - \mu + \mu x$ for several values of μ.

direct iteration of (1), which, as shown in [18], is equivalent to the Papoulis–Gerchberg algorithm. What is the value of μ that maximizes the convergence rate of (9)?

Let λ and $\mathbf{v}$ be an eigenvalue and the corresponding eigenvector of $\mathbf{S}$, respectively. Note that $1 - \mu + \lambda\mu$ is an eigenvalue of $\mathbf{S}_\mu$, corresponding to the same eigenvector. Thus, an eigenvalue λ of $\mathbf{S}$ is mapped into an eigenvalue $f_\mu(\lambda) = 1-\mu+\lambda\mu$ of $\mathbf{S}_\mu$. The function $|f_\mu(\lambda)|$ is sketched in Fig. 5 for several values of μ.

Values of μ in the range $(0, 1)$ slow the convergence rate relatively to $\mu = 1$, whereas values in $(1, 2)$ may or may not improve it. If the iteration converges for $\mu = 1$, it will converge for any other μ in $[0, 2]$, but this is not necessary for convergence. When $\mu > 2$, the iteration may or may not converge.

The asymptotic convergence rate of the method is dictated by the magnitude of the largest eigenvalue of $\mathbf{S}_\mu$, that is, by its spectral radius. The smaller the spectral radius, the faster the asymptotic convergence rate. The value of μ that minimizes the magnitude of the largest eigenvalue of $\mathbf{S}_\mu$ is given by the condition $f_\mu(\lambda_{\max}) = -f_\mu(\lambda_{\min})$. Thus, the optimum value of μ is given by

$$\mu_{\text{opt}} = \frac{2}{2 - \lambda_{\max} - \lambda_{\min}}. \tag{10}$$

This requires knowledge of the extreme eigenvalues of $\mathbf{S}$. In problems where the iterative method is a realistic alternative to direct inversion of $\mathbf{I} - \mathbf{S}$, finding the eigenvalues is likely to be a computationally demanding task. Even when the noniterative method can be applied, the iterative method allows for the inclusion of other possibly nonlinear constraints into the solution process in a very straightforward way.

The results given in this correspondence yield approximate values for the eigenvalues and, consequently, for the optimum value of μ, with negligible computational requirements.

For example, assume that $N = 300$ and $n = 30$. The sampling set is assumed to be U_2, for which $k = 4$. These are the same values that lead to Fig. 2. Let the data be lowpass with $m = 100$ nonzero harmonics, which means that $B = (2m+1)/N = 0.67$. By Theorem 2, since $Bk = 2.68$

$$0.5 \le \lambda_{\min} \le \lambda_{\max} \le 0.75.$$

Using Theorem 1

$$0.5 \le \lambda_{\min} \le 0.67, \qquad 0.67 \le \lambda_{\max} \le 0.75$$

in accordance with Fig. 2. It follows from (10) that

$$2.41 \le \mu_{\text{opt}} \le 3.45.$$

However, it is possible to do much better than this. Inspecting Figs. 1 and 2, it is apparent that for most values of m

$$\lambda_{\min} \approx \frac{\lfloor Bk \rfloor}{k}, \quad \lambda_{\max} \approx \frac{\lceil Bk \rceil}{k}.$$

In this example, $\lambda_{\min} \approx 0.5$ and $\lambda_{\max} \approx 0.75$, suggesting that

$$\mu_{\text{opt}} \approx \frac{2}{2 - 0.5 - 0.75} \approx 2.67$$

which is correct to two decimal places (the optimum value is approximately 2.666 68).

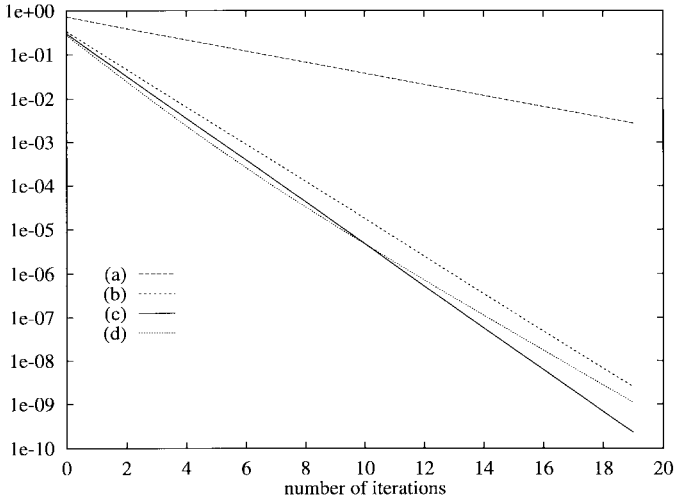

Fig. 6. Error evolution versus number of iterations $N = 300$, $n = 30$, $k = 4$, lowpass data, $2 \times 100 + 1$ nonzero harmonics. (a) $\mu = 1$. (b) $\mu = 2.6$. (c) $\mu = \mu_{\text{opt}} = 2.67$. (d) $\mu = 2.7$.

The error evolution of the algorithm (9) for several values of μ is depicted in Fig. 6. The set of missing samples is U_2.

The estimated values for μ are useful and sometimes quite close to the optimum values. This confirms the potential usefulness of the theoretical results presented in this paper for the computation of the optimum relaxation factors in this type of iterative reconstruction techniques.

B. Estimating the Minimum Interleaving Factor

Consider the transmission of a sampled signal packet by packet through a transmission channel (for example, the Ethernet). The recovery of lost or delayed packets can be accomplished using interpolation methods similar to those studied in this correspondence, but the question of stability is critical. Interleaving the samples among the packets helps to minimize the impact of lost packets but leads to delays that increase proportionally to the interleaving factor. Our results help in predicting the minimum interleaving factor.

Suppose that $N = 1024$ data samples with a normalized bandwidth $B = (2m+1)/N$ of 0.7 are to be transmitted. An interleaving factor of two (that is, transmitting the even and odd samples separately) leads to an interpolation problem similar to that considered in Theorem 2 with $k = 2$. The equations in (1) have to be solved for the vector of unknown samples $\mathbf{u}$, but in general, $\mathbf{h}$ is only approximately known (due to noise or poor estimation of the bandwidth B).

The bounds predicted by the theorem are 0 and 1, respectively, suggesting a large condition number for the matrix $\mathbf{S}$ and, consequently, low noise immunity. This is demonstrated in Fig. 7 when $\mathbf{S}$ is a 8×8 matrix, that is, for as few as $n = 8$ unknown samples.

The same happens when $k = 3$, but it is readily seen that when $k = 4$

$$\frac{1}{2} \le \lambda_{\min} \le \lambda_{\max} \le \frac{3}{4}$$

ensuring a condition number lower than 1.5. Under exactly the same conditions, the interpolation of $n = 200$ samples can be carried out

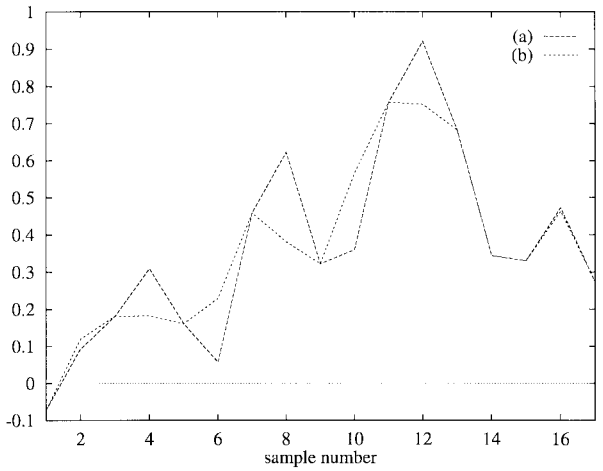

Fig. 7. Interpolating eight data samples in a record of $N = 1024$ samples with normalized bandwidth $B = (2m + 1)/N = 0.7$ using noisy data. (a) Original data. (b) Interpolated samples. Only 17 samples out of $N = 1024$ are shown. The indexes of the samples are multiples of two, and the bounds predicted by Theorem 2 are 0 and 1.

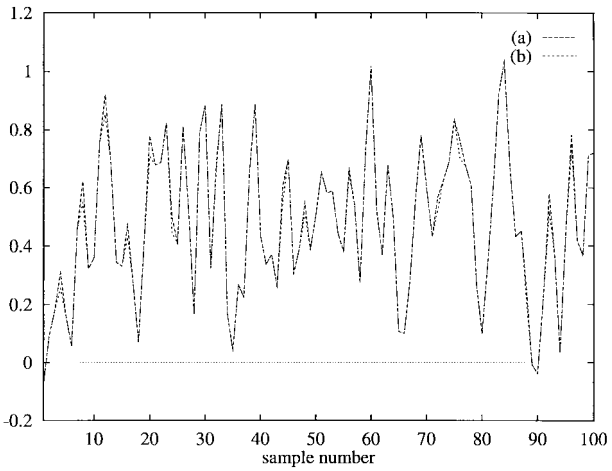

Fig. 8. Interpolating 200 data samples in a record of $N = 1024$ samples with normalized bandwidth $B = (2m + 1)/N = 0.7$ using the same data used in Fig. 7. (a) Original data. (b) Interpolated samples. Only 100 samples out of $N = 1024$ are shown. The indexes of the samples are multiples of four, and the bounds predicted by Theorem 2 are 0.5 and 0.75.

with much better results (Fig. 8). The total normalized error is now due to 200 samples instead of 8, but even so, it is five times lower than in the previous case.

V. Conclusion

The eigenvalues of a class of interpolation matrices depend very strongly on the sampling set involved. We have been able to explain this dependence and to supply bounds for the eigenvalues. The bounds are accurate and easy to find and explain the striking staircase-like behavior of the eigenvalues as a function of the number of nonzero harmonics.

The stability of the reconstruction problem and, therefore, the feasibility of the noniterative solution critically depends on the distribution of the missing samples. The results given help in evaluating the possibility of successful noniterative interpolation. When the noniterative method is not suitable or when other possibly nonlinear constraints are involved, it might be preferable to use iterative methods. In that case, the results help in estimating the convergence rates of the methods.

We have suggested that the transmission or archiving of data might be best accomplished by interleaving the samples. This maps the interpolation problem that results from the loss of a contiguous block of samples into a well-posed problem, which can be readily analyzed using the results given. Another possible application is the estimation of the optimum relaxation constants for iterative interpolation methods of minimum dimension and for the discrete Papoulis–Gerchberg algorithm.

References

[1] A. Papoulis, "A new algorithm in spectral analysis and bandlimited extrapolation," *IEEE Trans. Circuits Syst.*, vol. CAS-22, pp. 735–742, Sept. 1975.

[2] R. W. Gerchberg, "Super-resolution through error energy reduction," *Optica Acta*, vol. 21, no. 9, pp. 709-720, 1974.

[3] D. C. Youla, "Generalized image restoration by the method of alternating orthogonal projections," *IEEE Trans. Circuits Syst.*, vol. CAS-25, pp. 694–702, Sept. 1978.

[4] D. C. Youla and H. Webb, "Image restoration by the method of convex projections: Part 1—Theory," *IEEE Trans. Med. Imag.*, vol. MI-1, pp. 81-94, Oct. 1982.

[5] M. I. Sezan and H. Stark, "Image restoration by the method of convex projections: Part 2—Applications and numerical results," *IEEE Trans. Med. Imag.*, vol. MI-1, pp. 95–101, Oct. 1982.

[6] H. J. Trussel and M. R. Civanlar, "The feasible solution in signal restoration," *IEEE Trans. Acoust., Speech, Signal Processing*, vol. ASSP-31, pp. 201–212, Apr. 1984.

[7] R. G. Wiley, "Recovery of bandlimited signals from unequally spaced samples," *IEEE Trans. Commun.*, vol. COMM-26, pp. 135–137, Jan. 1978.

[8] F. A. Marvasti, M. Analoui, and M. Gamshadzahi, "Recovery of signals from nonuniform samples using iterative methods," *IEEE Trans. Signal Processing*, vol. 39, pp. 872–878, Apr. 1991.

[9] K. Yao, "Applications of reproducing kernel Hilbert spaces—Bandlimited signal models," *Inform. Contr.*, vol. 11, pp. 429-444, 1967.

[10] D. P. Kolba and T. W. Parks, "Optimal estimation for bandlimited signals including time domain considerations," *IEEE Trans. Acoust., Speech, Signal Processing*, vol. ASSP-31, pp. 113–122, Feb. 1983.

[11] R. J. Marks, II, "Restoring lost samples from an oversampled bandlimited signal," *IEEE Trans. Acoust., Speech, Signal Processing*, vol. ASSP-31, pp. 752–755, June 1983.

[12] P. Delsarte, A. J. E. M. Janssen, and L. B. Vries, "Discrete prolate spheroidal wave functions and interpolation," *SIAM J. Appl. Math.*, vol. 45, pp. 641–650, Aug. 1985.

[13] P. J. S. G. Ferreira, "Incomplete sampling series and the recovery of missing samples from oversampled bandlimited signals," *IEEE Trans. Signal Processing*, vol. 40, pp. 225–227, Jan. 1992.

[14] K. Gröchenig, "A discrete theory of irregular sampling," *Linear Algebra Appl.*, vol. 193, pp. 129–150, 1993.

[15] P. J. S. G. Ferreira, "Interpolation and the discrete Papoulis-Gerchberg algorithm," *IEEE Trans. Signal Processing*, vol. 42, pp. 2596–2606, Oct. 1994.

[16] T. Strohmer, "On discrete bandlimited signal extrapolation," in *Mathematical Analysis, Wavelets and Signal Processing: An International Conference on Mathematical Analysis and Signal Processing*, vol. 190, *Contemporary Mathematics*, M. E. H. Ismail, M. Z. Nashed, A. I. Zayed, and A. F. Ghaleb, Eds. Providence, RI: Amer. Math. Soc., 1995, pp. 323–337.

[17] P. J. S. G. Ferreira, "Interpolation in the time and frequency domains," *IEEE Signal Processing Lett.*, vol. 3, pp. 176–178, June 1996.

[18] ——, "Noniterative and faster iterative methods for interpolation and extrapolation," *IEEE Trans. Signal Processing*, vol. 42, pp. 3278–3282, Nov. 1994.

[19] ——, "The stability of a procedure for the recovery of lost samples in bandlimited signals," *Signal Process.*, vol. 40, no. 3, pp. 195–205, Dec. 1994.

[20] D. S. Chen and J. P. Allebach, "Analysis of error in reconstruction of two-dimensional signals from irregularly spaced samples," *IEEE Trans. Acoust., Speech, Signal Processing*, vol. ASSP-35, pp. 173–180, Feb. 1987.

[21] R. A. Horn and C. R. Johnson, *Matrix Analysis*. Cambridge, U.K.: Cambridge Univ. Press, 1990.